ADVANCED BIOSYSTEMS
www.adv-biosys.com

# Evaluation of Microfluidic Ceiling Designs for the Capture of Circulating Tumor Cells on a Microarray Platform

*Hui-Yu Liu, Claudia Koch, Anna Haller, Simon A. Joosse, Ravi Kumar, Michael J. Vellekoop, Ludwig J. Horst, Laura Keller, Anna Babayan, Antonio Virgilio Failla, Jana Jensen, Sven Peine, Franz Keplinger, Harald Fuchs, Klaus Pantel,* and Michael Hirtz**

**The capture of circulating tumor cells (CTCs) is still a challenging application for microfluidic chips, as these cells are rare and hidden in a huge background of blood cells. Here, different microfluidic ceiling designs in regard to their capture efficiency for CTCs in model experiments and more realistic conditions of blood samples spiked with a clinically relevant amount of tumor cells are evaluated. An optimized design for the capture platform that allows highly efficient recovery of CTCs from size-based pre-enriched samples under realistic conditions is obtained. Furthermore, the viability of captured tumor cells as well as single cell recovery for downstream genomic analysis is demonstrated. Additionally, the authors' findings underline the importance of evaluating rational design rules for microfluidic devices based on theoretical models by application-specific experiments.**

## 1. Introduction

Cancer remains the second most common cause of death worldwide.[1] As 90% of cancer-related deaths are caused by the formation of distant metastasis, understanding and preventing this decisive step of disease progression will be crucial for treatment improvement. Circulating tumor cells (CTCs) are cells released into the blood from the primary tumor and/or a metastatic lesion.[2–9] The detection of CTCs in patient blood is associated with reduced overall survival (OS) in various cancer types.[10–12]

Currently, cancer is primarily diagnosed by tissue biopsy, an invasive procedure that can lead to side effects such as bleeding and infection and is not feasible in all tissues (e.g., brain). Additionally, information gained by biopsy is limited to the site of tissue removal and furthermore cannot mirror the ever changing landscape of tumor evolution within a single patient. Blood-based analysis of CTCs could therefore function as a minimal invasive "liquid biopsy," allowing repeated sampling, a more holistic overview on disease development, and additional insights into the biology of metastasis formation.[13,14]

When analyzing CTCs, the main hurdle is the rarity of these cells in the background of millions of blood cells (≈1 CTC in $10^8$ blood cells).[15] To overcome this limitation, a multitude of assays have been and are currently under development.[3,16] However, so far only the CellSearch system (Menarini Silicon Biosystems, Italy) has gained approval for use in specific cancer

H.-Y. Liu, Dr. R. Kumar, Prof. H. Fuchs, Dr. M. Hirtz
Institute of Nanotechnology (INT) and Karlsruhe Nano Micro Facility (KNMF)
Karlsruhe Institute of Technology (KIT)
76344 Eggenstein-Leopoldshafen, Germany
E-mail: michael.hirtz@kit.edu

C. Koch, Dr. S. A. Joosse, L. J. Horst, Dr. L. Keller, Dr. A. Babayan, J. Jensen, Prof. K. Pantel
Department of Tumor Biology
University Medical Center Hamburg-Eppendorf
20246 Hamburg, Germany
E-mail: pantel@uke.de

The ORCID identification number(s) for the author(s) of this article can be found under https://doi.org/10.1002/adbi.201900162.



**DOI: 10.1002/adbi.201900162**

Dr. A. Haller, Prof. F. Keplinger
Institute of Sensor and Actuator Systems
TU Wien
1040 Vienna, Austria

Prof. M. J. Vellekoop
Institute for Microsensors
Microactuators and Microsystems (IMSAS)
Microsystems Center Bremen MCB
University of Bremen
28359 Bremen, Germany

Dr. A. V. Failla
Microscopy Imaging Facility (UMIF)
University Medical Center Hamburg-Eppendorf
20246 Hamburg, Germany

Dr. S. Peine
Department of Transfusion Medicine
University Medical Center Hamburg-Eppendorf
20246 Hamburg, Germany

Prof. H. Fuchs
Physical Institute and Center for Nanotechnology (CeNTech)
University of Münster
48149 Münster, Germany

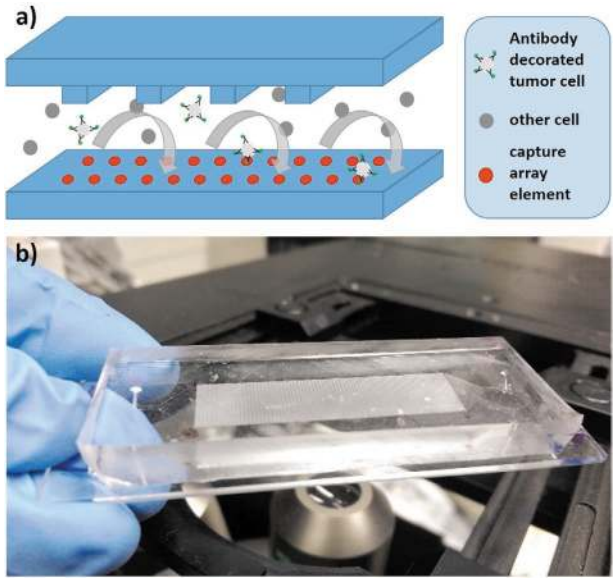


**Figure 1.** The CTC capture chip. a) Scheme of the capture principle. Antibody sensitized CTCs are captured on a microarray at the channel bottom, while other cells can pass the microfluidic chip. Structures in the channel ceiling ensure frequent contacts of cells with the microarray by inducing transverse flows. b) Photograph of a real microfluidic chip on an inverted microscope.

entities by the American Food and Drug Administration (FDA). While this system has been extensively validated, its limitation lies in the dependence of its CTC capture on EpCAM epithelial cell adhesion molecule (EpCAM).[17] While EpCAM is expressed on most epithelial tissues and therefore carcinoma cells, a growing amount of evidence is indicating that tumor cells undergo transition to a more mesenchymal state when initiating the metastatic cascade.[18,19] These cells downregulate epithelial markers such as EpCAM and therefore would most likely not be detected by the CellSearch system. This necessitates the development of promising and highly sensitive EpCAM-independent CTC detection platforms in order to isolate these highly aggressive CTC subtypes.

Recently, we developed a different approach in microfluidic CTC capture, based on a microfluidic encapsulated microarray.[20] Here, the CTC-containing samples are incubated with an antibody targeting the desired surface marker and then introduced into a microfluidic chip with a herringbone structured ceiling (**Figure 1**). The ceiling structure disrupts laminar streamlines and, thereby, enhances the number of cellular interactions with the reactive micropattern, comprising the specific binding sites for the CTCs. Thus, CTCs are immobilized on the array, while healthy cells leave the microfluidic chip on the outlet. The microarray within the microfluidic channel was printed via polymer pen lithography (PPL).[21] This technique combines aspects of microcontact printing and dip-pen nanolithography (DPN)[22] in a hybrid way and allows large area (several cm²) patterning,[23] especially for sensitive, bioactive molecules in gradients[24,25] and in a multiplexed fashion.[26–29] This allows also easy integration into microfluidic systems as we demonstrated for the above-mentioned application of CTC capture[20] and mast cell screening,[30] recently. In the application of these microarrays for CTC capture, the design of the microfluidic chip chamber ceiling is key to disrupt laminar streamlines in order to get CTCs into contact with the specific binding sites on the microarray. Structuring the channel ceiling with a staggered herringbone (SHB) design has proven to be an effective method to increase the number of cell–surface contacts. Originally, SHBs were proposed as a chaotic mixer for microchannels by Strook et al.[31] They showed that SHB mixers generate transverse flows that induce a stirring within the microchannel. These microvortices lead to stretching and folding of fluid volumes over the channel's cross section. Thereby, the diffusion length is reduced and, hence, mixing is significantly accelerated.

Stott et al. were among the first to apply the SHB mixer design to the isolation of CTCs.[32] Since then, SHBs have been utilized frequently for CTC capture.

The initial SHB design has been proposed and optimized for mixing purposes. For the purpose of capturing CTCs the aim is not mixing but transporting cells to a binding surface. On that account, Forbes et al. developed a computational model and a theoretical framework to optimize the geometry of the SHB design.[33] Recently, Lynn et al. have optimized the design of the SHB mixer for biosensing purposes as well, focusing on analyte transfer to the surface opposite the SHB grooves.[34,35] Considering the importance and benefits of theoretical and simulation results in the design process of microfluidics,[36] we set out to implement and compare these propositions in practice.

In the present work, we evaluate our chip platform with different SHB structures as suggested in the literature. As different herringbone structures are theoretically proposed for maximum efficiency of analyte delivery to active channel surface, we compare three different setups: design HA is the SHB design that we utilized in a previous publication,[20] design HB implements the suggestions of Forbes et al.,[33] and design HC follows the design rules that Lynn et al.[34,35] proposed. Additionally, the capture efficiency of a channel with smooth walls is included in the comparison.

## 2. Results and Discussions

### 2.1. The Chip Platform

In order to assess the influence of the different SHB structures in the chip ceiling (**Figure 2**) on the capture efficiency of the chip platform, three different designs were produced (**Table 1**, called ceiling type HA, HB, HC) and compared with each other as well as an unstructured microfluidic channel. The herringbone is composed of a series of chevrons with a long and a short groove. The short groove covers one third of the symmetry width $w_{hb}$ and the long groove covers the remaining two thirds. The angle between grooves $\theta_{hb}$ is 90° and the angle with the channel wall $\theta_c$ is 45°.

Each chevron is $w_{hb}$ wide and placed side by side to cover the complete channel width $w_c$. Grooves are $w_g$ wide, $h_g$ high and separated with a pitch $\Lambda$. The height of the smooth part of the channel is $h_c$. The shape of the SHBs is varied as a function of the axial position in the microchannel. After $N_g$ chevrons per part-cycle, they are staggered by an offset $\delta_g$.

Publications by Forbes et al. and Lynn et al. on geometrical optimization of the SHB design provide design guidelines to enhance

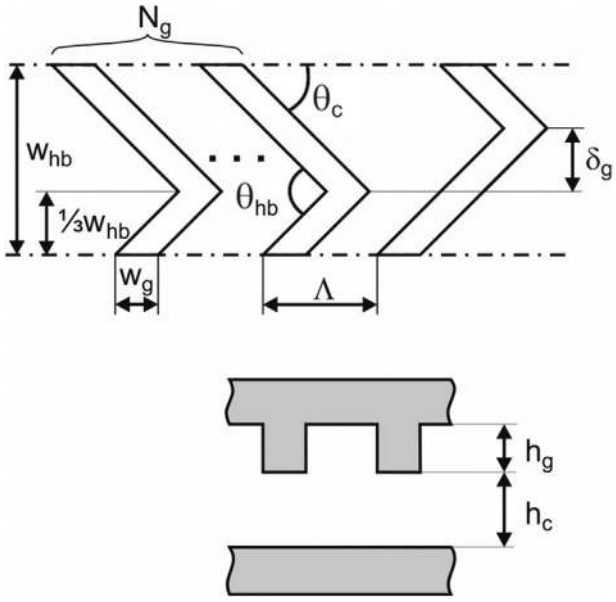


**Figure 2.** Scheme of chip ceilings. Schematic of a staggered herringbone design, illustrating the geometrical parameters: channel height $h_c$, groove height $h_g$, groove width $w_g$, groove pitch $\Lambda$, symmetry width $w_{HR}$, number of chevrons per part-cycle $N_g$ and offset per cycle $\delta_g$.

the number of particle–surface interactions in SHBs.[33–35] However, the results published by these two groups contradict each other in the following parameters: groove width $w_g$, groove height $h_g$, and symmetry width $w_{hb}$. Nevertheless, they agree that the groove pitch $\Lambda$ has little or no effect on capture efficiency.

Forbes et al. focus on the groove-to-channel relative hydraulic resistance and suggest that SHBs with wide and deep grooves enhance the number of interactions at the surface opposite to the SHBs.[33] Consequently, the geometrical parameters, labeled HB in Table 1, were chosen.

Lynn et al. conclude that the ratio $h_g/h_c$ is one of the most important design parameters and should be in the region of $1.2 < h_g/h_c$.[34,35] As the channel height is 50 µm, the groove height was chosen to be 75 µm, resulting in $h_g/h_c = 1.5$. The geometrical parameters following these suggestions are given in Table 1, labeled HC.

To find the optimal SHB structure for CTCs capture purposes, the designs HB and HC were fabricated and their capture efficiency was evaluated experimentally. Additionally, the SHB design that was utilized in a previous publication by our group, labeled HA, and a smooth channel with height $h_c = 150$ µm were included in the comparison.

All designs have the following parameters in common: complete channel width $w_c = 9600$ µm, number of grooves per part-cycle $N_g = 5$, angle of herringbone $\theta_{hb} = 90°$ and the angle with channel wall $\theta_c = 45°$.

**Table 1.** Design parameters of the staggered herringbone ceiling.

| Geometrical parameter | HA [µm][a)] | HB [µm][b)] | HC [µm][c)] |
|---|---|---|---|
| Channel height $h_c$ | 50 | 50 | 50 |
| Groove height $h_g$ | 50 | 150 | 75 |
| Groove width $w_g$ | 100 | 125 | 50 |
| Groove pitch $\Lambda$ | 100 | 200 | 100 |
| Symmetry width $w_{hb}$ | 300 | 500 | 150 |
| Offset per cycle $\delta_g$ | 100 | 500 | 150 |

[a)]As used in our previous publication[20]; [b)]Following design rules by Forbes et al.[33]; [c)]Following design rules by Lynn et al.[34,35]

### 2.2. Performance in Tumor Cell Capture

To compare the performance of the different ceiling types for the microarray chip platform, trials with different concentrations of cancer cell line cells were performed. Mixtures of 100 and 10 000 biotinylated cancer cells (MCF-7) and $10^4$ to $10^6$ non-biotinylated cancer cells were tested on the different microfluidic chips (different pattern pitches and chamber designs). A streptavidin-patterned chip surface with an array feature pitch of 50 µm combined with the SHB design type HC showed the highest capture rate among the different tested combinations (**Figure 3**c and Table S1, Supporting Information).

Statistical analyses showed that both the ceiling type ($p = 0.0015$) and pattern structure ($p < 0.0001$) had a significant impact on the capture rate, with a possible interaction between the two ($p = 0.0089$), cell suspension concentration was also significantly correlated to the capturing rate ($p = 0.044$), but not as strong and was therefore not further considered. Pairwise analyses indicated that ceiling type HB was outperformed by HA with 29.8% (95% CI: [10.1, 49.4], $p = 0.0019$) and HC with 30.8% (95% CI: [9.2, 52.3], $p = 0.0034$), whereas the smooth ceiling type was not highly statistically different compared to the other three ($p > 0.005$). The pattern structure of 50 µm showed a 25.2% better mean capturing than the 25 µm (95% CI: [11.0, 39.5], $p = 0.0006$) and a 28% better capturing than the homogeneous pattern structure (95% CI: [13.1, 42.9], $p = 0.0003$). Interaction effects between the ceiling type and pattern structure confirmed that 60% higher mean recovery rates could be achieved with the 50 µm herringbone HA and HC compared to the smooth type or HB ($p < 0.005$). No statistically significant difference in the mean rate of capture was detected between ceiling types HA and HC at the same pattern structure.

Based on these results, a pattern pitch of 50 µm was chosen (as here the overall highest recovery performance was found) for subsequent experiments to allow more in-depth comparison across the different chip designs under "mock" blood sample conditions. Here, 100 cancer cell line cells (MCF-7) were spiked into blood samples of healthy donors (containing around $5 \times 10^9$ cells $mL^{-1}$). As described previously,[20] these "mock" blood samples were subjected to a size-based pre-enrichment by the Parsortix system. This workflow allows for removal of a large fraction of healthy white blood cells and erythrocyte background by size exclusion.[37] After pre-enrichment, the remaining cells (1500–6000 dependent on donor)[38,39] were sensitized by biotinylated-anti-EpCAM antibodies and pumped into the respective chip. Following additional staining with fluorescently labeled antibodies (secondary anti-mouse, DAPI, CD45), the tumor cells bound on the chip surface were manually counted with an upright fluorescence microscope.

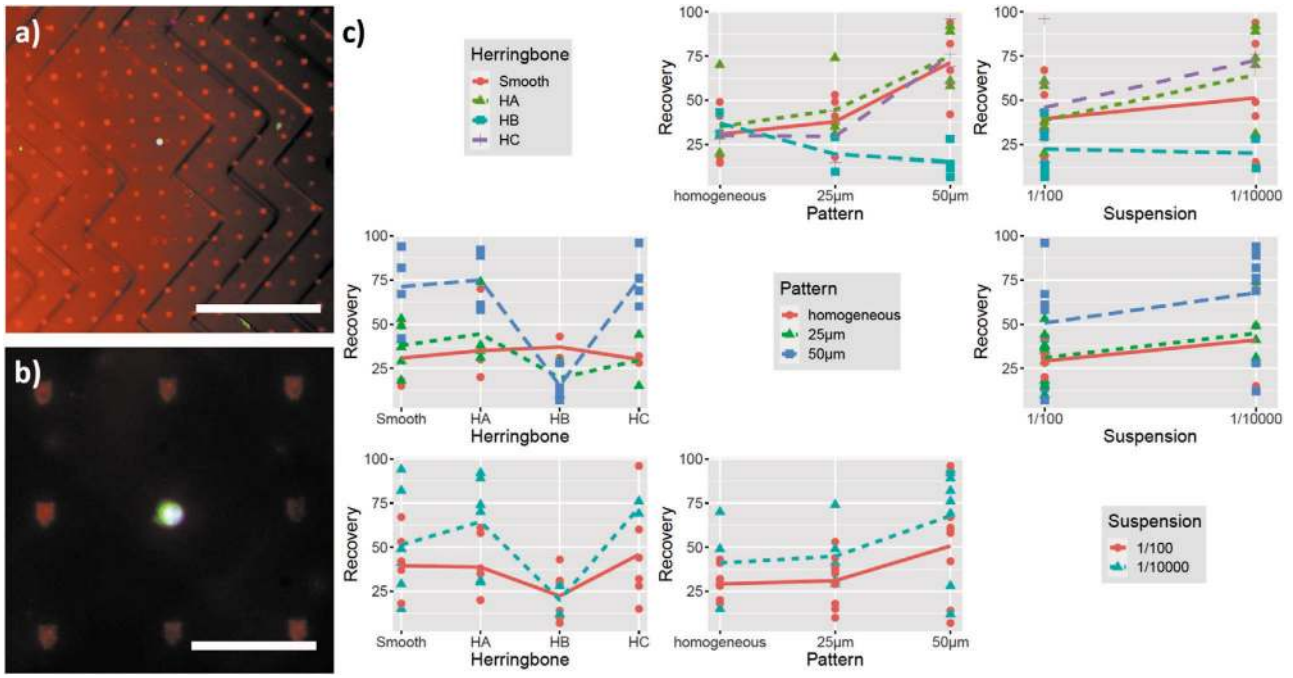


**Figure 3.** Captured cells on a microarray and correlation matrix of examined chip and pattern designs. a) Single captured CTC on a microarray. The translucent herringbone ceiling structure is visible. Scale bar equals 250 µm. b) Close-up of the cell. Note the low background of other cells and the co-localization of microarray pattern with the captured CTC. Scale bar equals 50 µm. c) Correlation matrix showing the recovery of tumor cells under the different experimental conditions of the ceiling type (Herringbone, top row), pattern design (Pattern, center row), and the cell suspension concentration (Suspension, bottom row).

Representative images of stained tumor cells captured on the streptavidin dots of the chip are shown in Figure 3a,b. As median recovery for the different ceiling types, 10% for smooth, 13% for type HA, 3% for type HB, and 38% for type HC, respectively, were obtained (**Figure 4**). The standard deviations (SD) measured here represent an accumulation of the SD of both the pre-enrichment via Parsortix, and the actual chip processing. The SD of the HC chip appears to be higher than in the other chips which is most likely due to the fact that more cells can be detected with this compared to the other chip types (e.g., HB). It is natural for the variation in recovery to decrease the closer the recovery is to zero. Since the recovery obtained with the HC chip among the different experiments is normally distributed, the results remain highly trustworthy. Nonetheless, we will strive to further improve the reproducibility in future experiments. Statistical analysis shows a significant difference in the mean recovery rate between the ceiling types ($p = 0.0006$). Type HC outperformed the smooth type with 30.3% (95% CI: [11.8, 48.7], $p = 0.0025$), type HA with 22.9% (95% CI: [4.5, 41.4], $p = 0.015$), and type HB with 34.6% (95% CI: [16.1, 53.1], $p = 0.0009$). No statistically significant difference was detected between type HA and HB ($p = 0.35$), HA and smooth ($p = 0.70$), and HB and smooth ($p = 0.92$). Taken together, the HC type (designed as suggested by the Lynn et al. rules for maximization of the number of surface interactions)[34,35] shows the overall best recovery performance and significantly improves on our previously used[20] HA type and the HB type (based on the alternative design rules suggested by Forbes et al.).[33] Current standard approaches used downstream of the Parsortix system, such as the classical ICC staining on cytospins (pan-cytokeratin, CD45, and DAPI) reach an average recovery of (32 ± 4)% using MCF-7 cells and the same Parsortix separation protocol (Table S2, Supporting Information). Of note, a broader

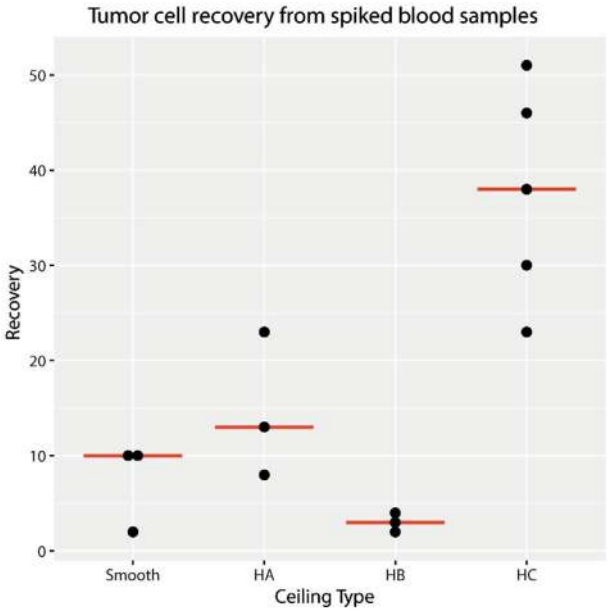


**Figure 4.** Capture efficiency in spiked blood samples. Ceiling type HC (median recovery 38%) outperforms the other ceiling types significantly. No statistically significant differences were detected between the smooth ceiling (median recovery 10%) and ceiling types HA (median recovery 13%) and HB (median recovery 3%).

discussion and comparison of different CTC isolation systems can be found in the literature.[3,40,41] Factoring in these losses in the upstream processing and assuming that the Parsortix separation is the main point these occur (neglecting the contribution of the cytospin process), the HC system would have a (theoretical) recovery of 118% (excess of 100% probably reflecting the neglected losses during cytospin that cannot easily be deconvoluted). This estimation shows that the HC system has a virtually full recovery of cells obtained in the upstream process.

Sample purity represents a crucial factor of CTC isolation techniques. However, it is most relevant when no further discrimination between target cells (CTCs) and cellular background (e.g., leucocytes) takes place and when samples are furthermore subjected to bulk analysis. In our case, potential target cells on the chip are fluorescently stained using established CTC markers as well as leucocyte exclusion markers allowing apt differentiation between both cellular populations. The microarray features themselves provide a strong reference to distinguish targets and unspecific background by co-localization of targets with the array features (Figure S1, Supporting Information). Furthermore, analysis of CTCs identified on the chip is based on single cell isolation and not bulk analysis, therefore circumventing the need for even higher purity in samples. Overall, leukocyte background remained under 500 nucleated cells for all blood samples tested (data not shown). Sample pre-enrichment via Parsortix was shown to result in a residual count of 200–800 nucleated cells per mL of processed blood,[38] translating to 1500–6000 nucleated cells post size-based enrichment of a standard 7.5 mL EDTA blood tube. This leukocyte background is known to be donor dependent.[39] Considering these numbers, our chip achieves a minimal further sample purification of threefold and maximum additional sample purification of over 12-fold.

### 2.3. Cell Viability following Tumor Cell Capture

Although progress has been made during recent years, culturing CTCs from patient blood ex vivo remains challenging to this day. So far only very few CTC-derived cell lines could successfully be established,[42–44] limiting the functional understanding of these cells. The viability of captured tumor cells following enrichment or isolation represents a vital prerequisite for successful transient or permanent culture. A cell viability of 99% was demonstrated for cells separated by the Parsortix system in earlier studies[37,45] indicating that processing of samples using this technology has a negligible effect on cell viability. For this reason, in this study, we focused on assessing the impact of chip processing in itself on cell viability. To test the viability of cells passed through our chip, we sensitized breast cancer cell line cells (MDA-MB-468) with biotinylated-anti-EpCAM antibodies and captured them on the streptavidin surface according to standard protocol. Subsequently, dead cells were stained directly within the chip using 0.4% trypan blue. Cells were screened and images were taken in bright field (**Figure 5**). The vast majority of MDA-MB-468 cells captured on the chip remained viable showing no evident trypan blue staining. In total, around 10% of dead and 90% of viable cells were detected. Combined with the possibility of removing the PDMS microfluidic chamber and placing the glass slide containing the immobilized tumor cells directly into a petri dish for culture, this promising result of 90% viable tumor cells following enrichment with the chip, suggests good starting conditions for future CTC culture.

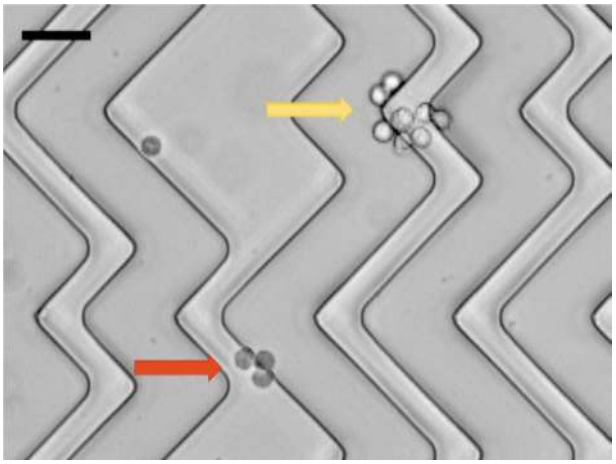

**Figure 5.** Viability staining of captured cancer cell line cells. Exemplary image of MDA-MB-468 cells taken in bright field, following capture on the chip. An image containing trypan blue stained cells was chosen, while representing the minority, to demonstrate staining efficiency. The herringbone structure of the microfluidic chamber is visible as grey waves. Black scale bar represents 50 µm. Viable cells indicated by yellow arrow and dead cells stained by trypan blue indicated by red arrow.

### 2.4. Feasibility of the Workflow for Downstream Genomic Analysis of Single Tumor Cells

In order to test the compatibility of our chip workflow with downstream molecular single cell analysis, tumor cell line cells (MCF-7 and SK-MEL-28 cell line cells) were spiked into a background of peripheral blood mononuclear cells (PBMCs), captured on the chip, stained with immunofluorescent markers, and picked by micromanipulation for subsequent whole genome amplification (WGA). As negative control for the WGA, PBS pipetted from the same chip was used, whereas human reference DNA was employed as positive control. Ten MCF-7 and 10 SK-MEL-28 single cells were used for WGA of which 50% (5/10) of the genomes could be successfully amplified at highest quality (4/4 bands) for each cell line, as determined by a multiplex PCR against four different fragments of the human *GAPDH* gene (Figure S2, Supporting Information). An additional single SK-MEL-28 cell showed 1/4 quality control bands, indicating sufficient DNA quality for PCR or Sanger sequencing applications. These results demonstrate compatibility of the CTC chip isolation workflow with micromanipulation and WGA of cells of interest for downstream applications.

## 3. Conclusion

In this study, we investigated the influence of ceiling structure and target cell concentration on the capture efficiency of

our CTC capture platform based on microarrays. Trialing different design rules, we were able to greatly enhance the capture rate in comparison to our previous design. Compared to other tandem systems such as pre-enrichment by Parsortix and detection via staining on cytospins, our system is performing on a competitive level. Additionally, when the cell loss during pre-enrichment is factored in to enable comparison to other microfluidic chips described in the literature working not as tandem device,[32,46–49] this chip platform is estimated to have a near full recovery. To further allow the chip platform to unfold its unique potential, necessary pre-enrichment steps will need to be addressed and refined in future studies. Furthermore, the chip platform is suitable for live cell capture, as demonstrated by a 90% viability of captured cells. These could potentially be used for cell culture and further downstream genomic analysis. Microfluidic systems have been shown to outperform the "gold standard" CellSearch device on multiple occasions.[50–56] However, it is important to keep in mind, that most of these platforms utilize additional or alternative markers for CTC isolation[50–52] or work with antibody cocktails,[53,54] thereby complicating the direct comparison of both approaches. At this point in time, we chose EpCAM as a target for CTC capture on our chip in order to demonstrate the feasibility of our workflow using a well-established marker and to allow for future direct comparison to the CellSearch. While we demonstrate capturing by EpCAM, it should be noted that the design allows free exchange of used antibody without need for other changes in setup or operations, thus allowing virtual free choice of target marker. Overall, the optimized chip platform is a very promising tool enabling future studies on CTCs and other potential diagnostic applications.

## 4. Experimental Section

*Microarray Printing*: The microarray was printed according to the procedures published previously.[20] Briefly, the polydimethylsiloxane (PDMS, ABCR, Karlsruhe, Germany) stamps were prepared from silicon master (50 µm and 100 µm pitch) which was previously fabricated by photolithography and chemical etching process. The PDMS stamps were treated with oxygen plasma (0.2 mbar, 100 W, 10 sccm $O_2$, 2 min, ATTO system, Diener electronics, Germany) before inking to render the surface hydrophilic. The stamps were spin coated (3000 rpm, 30 s) for homogenous coating with the ink of biotin-4-fluorescein (Sigma-Aldrich, Germany). The stamp was first glued with two component epoxy resin adhesive (UHU, Germany) to a microscopic glass slide, then the whole glass slide was glued to the bar of a custom made holder and rested for 2 min to dry. The stamp holder was then attached to the NLP2000 system (NanoInk Inc., USA) that offers a piezo-driven stage, able to perform micro-printing. As substrate, the microscopy glass slides (Menzel Gläser, Germany) were sonicated for 10 min each in chloroform, isopropanol, and deionized water. The cleaned microscopy slides were then immersed in a solution of 3% bovine serum albumin (BSA, Sigma-Aldrich, Germany) in phosphate buffered saline (PBS, Sigma-Aldrich, Germany) overnight. The slides were then dipped ten times in ultrapure water (18.2 MΩcm) to remove the extra BSA and subsequently dried with nitrogen. After this, the BSA-coated substrates were ready to use for the microarray printing. The plasma-cleaned PDMS stamp of area $10 \times 10$ mm$^2$ was levelled[29] and contacted once to the substrate for printing patterns having 50 µm distance between ink dots. Then the stamp was moved by 10 mm and contacted again to obtain a large area biotin dots pattern next to the already printed area. This process of printing was repeated four times, resulting in a total area of $40 \times 10$ mm$^2$. Printing was done at 50–70% relative humidity and dwell time of 1–10 s. The biotin-4-fluorescein micropatterns were then immediately immobilized by a UV lamp (365 nm, Technotray CU, Heraeus, Germany) for 15 min after printing (bleaching the fluorescein and in the process photochemically binding it to the BSA) and stored at room temperature until use.

*Fabrication of the Staggered Herringbone Chip*: The microfluidic chips were fabricated in a three-step process. Initially, a mold was produced, that exhibits the inverse of the microfluidic channel including the SHB structure, by photolithographically patterning two layers of a negative photoresist (SU-8, MicroChem, USA) on a silicon wafer. A 50 µm thick layer of SU-8 was spin coated, followed by a soft bake. This layer was exposed to form the negative of the channel without grooves. After post exposure bake and before developing the photoresist, a second layer of SU-8 was spin coated and soft baked. Depending on the design, the rotational speed was altered to reach the groove height. The SU-8 was then exposed to form the negative of the herringbone-shaped channel ceiling. Following another post exposure bake, the pattern was developed. Finished master templates can be reused for replica molding without any noticeable degradation in performance.

In the second step, PDMS prepolymer and its curing agent (Sylgard, 184, Dow Corning, USA) were mixed at 10:1 weight ratio, degassed, and casted to replicate the molding template. After curing on a hot plate (70 °C, 4 h), the PDMS replica was carefully released from the mold. Fluidic inlet and outlet ports were punched with a syringe needle.

In the third step, the SHB chip was bonded onto the microarray glass slide by oxygen plasma treatment to form a microfluidic flow chamber. An additional PDMS layer was placed onto the micropattern to protect it during plasma exposure. Finally, tubings (material: PEEK, outer diameter ø = 790 µm, inner diameter ø = 250 µm, Lab-Smith, USA) were fitted into the punched fluid connector holes to finish the microfluidic chip featuring a direct syringe interface (see Figure 1b for a photograph of a completed chip). The smooth channel comparison chips were produced by attaching a commercially available smooth channel with height $h_c$ = 150 µm (sticky-Slide I 0.1 Luer, ibidi, Germany) onto a microarray glass.

*Preparation and Connection of Microfluidic Chips*: The connection procedure for the SHB chips was performed according to the procedures published previously.[20] The ibidi chips (with unstructured channel) were prepared as follows: To provide a steady flow, a 1 mL syringe (BD Bioscience, USA) in a syringe pump (NE-1002X, Fisher Scientific, USA) was directly inserted into the inlet port of an ibidi chip and the outlet port was connected to a tube by a male Luer lock connector (ibidi, Germany) for waste collection. In order to rinse the whole chamber and to block unspecific protein binding at the channel walls before use, 100 µL of PBS with 1% w/V BSA (Sigma-Aldrich, Germany) and 1% v/v Tween20 (Fluka Analytical, Germany) was pumped into the chip and incubated for 15 min. Then the entire solution in the chamber was replaced with 200 µL of cy3 labeled streptavidin in PBS (0.5% v/v). The binding of streptavidin on the biotin patterns was allowed for 20 min. Finally, the chip was flushed with 500 µL PBS to remove excess streptavidin and rendered ready to use.

*Standard Cell Culture*: MCF-7, MDA-MB-468 breast cancer cell line cells, and SKMEL28 melanoma cell line cells, were cultured in Dulbecco's modified Eagle's medium (Life Technologies, Germany) supplemented with 10% calf bovine serum (Sigma-Aldrich, Germany), 1% L-glutamine (Gibco—Life Technologies, USA), and 1% penicillin/streptomycin (Gibco—Life Technologies, USA) under standard cell culture conditions (37 °C and 5% $CO_2$).

*Preparation of Cell Culture Cells for Chip Experiments*: $1 \times 10^5$ MCF-7 cells were sensitized with 0.5 µg mL$^{-1}$ of biotinylated-anti-EpCAM antibody (VU-1D9, Abcam, UK) in a shaker (Eppendorf Thermomixer Comfort, Hamburg, Germany) revolving at 300 rpm at 37 °C for 40 min. The biotinylated cells were then washed with PBS to remove unbound antibody. 100 biotinylated MCF-7 cells were manually counted and mixed with ≈10000 (based on cell concentration) untreated MCF-7 cells as negative controls in a total volume of 300 µL of pre-warmed 0.1% BSA in PBS buffer (37 °C). This mixture was used to test and

compare the recovery of different microfluidic chip designs. For manual spiking, 10 µL of cell culture cell suspension were applied to a petri dish containing 1× PBS. The petri dish was then placed under a light microscope and focused on in 5× or 10× magnification. Using a 10 µL Eppendorf pipette, single cells were manually pipetted into the pipette tip and transferred to the respective background cell solution.

*Preparation of "Mock" Blood Samples for Chip Experiments*: 7.5 mL of whole blood was collected from healthy donors in accordance to the World Medical Association Declaration of Helsinki and the guidelines for experimentation with human materials by the Chambers of Physicians of the State of Hamburg ("Hamburger Ärztekammer"). Blood was spiked with 100 manually counted MCF-7 cells to mimic clinical cancer patient samples. Manually spiked cells were handled as mentioned above. These "mock" blood samples were pre-enriched using the size-based Parsortix system (ANGLE plc) before applying our microfluidic chip assay. The function and handling of the Parsortix system has been described in detail in prior publications.[37] The total amount of cells remaining following Parsortix enrichment was between 1500 and 6000 dependent on donor.[38,39] Cells were harvested into a 1.5 mL reaction tube and centrifuged at 500× g, for 5 min to replace the PBS with pre-warmed 0.1% BSA in PBS buffer (37 °C). The pre-enriched cells were then incubated with 0.5 µg $mL^{-1}$ of biotinylated-anti-EpCAM antibody (VU-1D9, Abcam, UK) in a shaker (Eppendorf Thermomixer Comfort, Hamburg, Germany) revolving at 300 rpm at 37 °C for 40 min. Following antibody incubation, the cells were centrifuged at 500 × *g*, for 5 min to remove excess antibody and subsequently re-suspended in 200 µL of 0.1% BSA/PBS (37 °C). The sensitized pre-enriched cell fraction was then pumped into different microfluidic chip designs.

*Capture and Staining of Tumor Cells on the Chip*: The process of running the microfluidic chip has been described in detail in our prior publication.[20] In brief, the sensitized cells were pipetted into a 1 mL syringe (BD Bioscience, USA) which was connected to the device. A syringe pump passes the cells into the chip with a steady flow rate of 20 µL $min^{-1}$. During this time, the chips were placed on a hot plate (Heidolph MR Hei-Tec, Schwabach, Germany) set to 37 °C. After a 15 min of incubation, the captured cells were fixed with 0.5% paraformaldehyde for 15 min and stained with DAPI (1:1000, Sigma-Aldrich, Germany) and a secondary fluorescently labeled antibody (anti-mouse Alexa488-fluorophore 1:200, Abcam) for 30 min. Finally, chips were flushed with PBS (500 µL, 50 µL $min^{-1}$) and transferred to microscopy for readout.

*Readout of the Chips and Analysis*: The entire chip area containing the immobilized tumor cells was manually scanned with a 10× objective on an upright fluorescence microscope (Eclipse 80i, Nikon Instruments Europe B.V., Germany) and the number of stained tumor cells bound to streptavidin dots was obtained by manual counting.

*Viability Assessment of Captured Tumor Cells*: Viability of tumor cells captured by the chip was assessed by trypan blue staining. Trypan blue is an azo dye that is only able to enter through the cell membrane of dead cells, staining them in a dark blue color, while live cells remain unstained. The blue color was visible by standard light microscopy. $1 \times 10^6$ MDA-MB-468 cells (without leucocyte background) were processed through the chip according to standard protocol in a HC-type chip. A temperature of 37 °C was strictly maintained for the entire duration of the chip run and all used fluids. Following an incubation period of 15 min, 80 µL of 0.4% trypan blue (Sigma-Aldrich, Germany) were passed through the chip at a flow rate of 1.2 mL $h^{-1}$. Subsequently, excess dye was washed out with 500 µL of PBS and the chip was analyzed by bright-field microscopy (Axiovert 200M, Zeiss, Germany). Random areas of the chip were selected for imaging (Software: Axiovision 4.8.2) and to assess the number of dead cells in relation to viable cells.

*Single Cell Manipulation and Downstream Analyses*: In order to test the efficiency of the proposed system for downstream genomic analyses, the complete workflow was tested for its compatibility with WGA and molecular characterization of the genomic material. In brief, breast cancer cell line MCF-7 and melanoma cell line SK-MEL-28 cells were transferred into a background of 60 000 PBMCs and sensitized with biotinylated-anti-EpCAM antibody (VU-1D9, Abcam, UK) or the combination of biotinylated MCAM (REA773, Miltenyi, Germany) and NG2 (EP1, Miltenyi, Germany) antibodies, respectively. Next, the enrichment and staining of tumor cells was performed in a HC-type chip as described above. MCF-7 cells were stained with pan-keratin antibody coupled to Alexa 488 (clone AE1/AE3, eBioSciences, USA), and SK-MEL-28 cells were stained with anti-MCAM (clone 541-10B2, Miltenyi, Germany) and anti-NG2 (LMH2, Novus Biological, USA) antibodies both coupled to PhycoErythrin. In both cases DAPI nuclear staining was performed. The chips were opened by removing the microfluidic chamber from the printed slide by cutting the PDMS layer with a scalpel. Single tumor cells ($n$ = 10 for each cell line) were isolated from the pattern by micromanipulation, individually transferred into 0.2 mL PCR tubes and immediately frozen at −80 °C. Next, WGA was performed using the Ampli1 WGA kit (Menarini Silicon Biosystems, Italy) according to the manufacturer's recommendations. The quality of the amplified DNA was assessed by multiplex PCR producing 96, 108–166, 299, and 614 bp fragments from target sites in the *GAPDH* gene using the Ampli1 QC Kit (Menarini Silicon Biosystems, Italy). PCR products were analyzed in a 1.2% agarose TAE ethidium bromide stained gel.

*Statistical Analysis*: Statistical analyses were performed in R.[57] ANOVA followed by Tukey's pairwise analyses were employed to test the capture efficiency of the different ceiling type structures and patterns under the two different cell concentration conditions, as well as to test the recovery of spiking experiments using the different SHB structures. $p$-values of $\leq 0.005$ were considered statistically significant as recommended by novel statistical guidelines.[58]

## Supporting Information

Supporting Information is available from the Wiley Online Library or from the author.

## Acknowledgements

H.-Y.L., C.K., and A.H. contributed equally to this work. The authors thank Prof. Andrew C. Cato (ITG, KIT) for access to his lab and fruitful discussions. This work was partly carried out with the support of the Karlsruhe Nano Micro Facility (KNMF, www.knmf.kit.edu), a Helmholtz Research Infrastructure at Karlsruhe Institute of Technology (KIT, www.kit.edu) and supported by the European Research Council (ERC) in a proof of concept grant.

## Conflict of Interest

H.F., K.P., and M.H. have applied for a patent regarding the microarray capture platform (WO 2016/128125 A1).

## Keywords

breast cancer, circulating tumor cells, microfluidics, polymer pen lithography, staggered herringbone design

Received: July 25, 2019
Revised: November 26, 2019
Published online: December 23, 2019

[1] WHO cancer fact sheet,http://www.who.int/news-room/fact-sheets/detail/cancer (accessed: November, 2019).
[2] C. Chaffer, R. Weinberg, *Science* **2011**, *331*, 1559.

[3] S. A. Joosse, T. M. Gorges, K. Pantel, *EMBO Mol. Med.* **2015**, *7*, 1.
[4] S. Riethdorf, V. Müller, S. Loibl, V. Nekljudova, K. Weber, J. Huober, T. Fehm, I. Schrader, J. Hilfrich, F. Holms, H. Tesch, C. Schem, G. Von Minckwitz, M. Untch, K. Pantel, *Clin. Cancer Res.* **2017**, *23*, 5384.
[5] F.-C. Bidard, S. Michiels, S. Riethdorf, V. Mueller, L. J. Esserman, A. Lucci, B. Naume, J. Horiguchi, R. Gisbert-Criado, S. Sleijfer, M. Toi, J. A. Garcia-Saenz, A. Hartkopf, D. Generali, F. Rothé, J. Smerage, L. Muinelo-Romay, J. Stebbing, P. Viens, M. J. M. Magbanua, C. S. Hall, O. Engebraaten, D. Takata, J. Vidal-Martínez, W. Onstenk, N. Fujisawa, E. Diaz-Rubio, F.-A. Taran, M. R. Cappelletti, M. Ignatiadis, et al., *JNCI, J. Natl. Cancer Inst.* **2018**, *110*, 560.
[6] F.-C. Bidard, D. J. Peeters, T. Fehm, F. Nolé, R. Gisbert-Criado, D. Mavroudis, S. Grisanti, D. Generali, J. A. Garcia-Saenz, J. Stebbing, C. Caldas, P. Gazzaniga, L. Manso, R. Zamarchi, A. F. de Lascoiti, L. De Mattos-Arruda, M. Ignatiadis, R. Lebofsky, S. J. van Laere, F. Meier-Stiegen, M.-T. Sandri, J. Vidal-Martinez, E. Politaki, F. Consoli, A. Bottini, E. Diaz-Rubio, J. Krell, S.-J. Dawson, C. Raimondi, A. Rutten, et al., *Lancet Oncol.* **2014**, *15*, 406.
[7] H. I. Scher, G. Heller, A. Molina, G. Attard, D. C. Danila, X. Jia, W. Peng, S. K. Sandhu, D. Olmos, R. Riisnaes, R. McCormack, T. Burzykowski, T. Kheoh, M. Fleisher, M. Buyse, J. S. de Bono, *J. Clin. Oncol.* **2015**, *33*, 1348.
[8] H. I. Scher, R. P. Graf, N. A. Schreiber, B. McLaughlin, D. Lu, J. Louw, D. C. Danila, L. Dugan, A. Johnson, G. Heller, M. Fleisher, R. Dittamore, *Eur. Urol.* **2017**, *71*, 874.
[9] M. G. Krebs, R. Sloane, L. Priest, L. Lancashire, J.-M. Hou, A. Greystoke, T. H. Ward, R. Ferraldeschi, A. Hughes, G. Clack, M. Ranson, C. Dive, F. H. Blackhall, *J. Clin. Oncol.* **2011**, *29*, 1556.
[10] M. Cristofanilli, G. Budd, *N. Engl. J. Med.* **2004**, *351*, 781.
[11] S. J. Cohen, C. J. A. Punt, N. Iannotti, B. H. Saidman, K. D. Sabbath, N. Y. Gabrail, J. Picus, M. Morse, E. Mitchell, M. C. Miller, G. V. Doyle, H. Tissing, L. W. M. M. Terstappen, N. J. Meropol, *J. Clin. Oncol.* **2008**, *26*, 3213.
[12] J. S. De Bono, H. I. Scher, R. B. Montgomery, C. Parker, M. C. Miller, H. Tissing, G. V. Doyle, L. W. W. M. Terstappen, K. J. Pienta, D. Raghavan, *Clin. Cancer Res.* **2008**, *14*, 6302.
[13] C. Alix-Panabières, K. Pantel, *Cancer Discovery* **2016**, *6*, 479.
[14] A. Bardelli, K. Pantel, *Cancer Cell* **2017**, *31*, 172.
[15] C. Alix-Panabières, K. Pantel, *Nat. Rev. Cancer* **2014**, *14*, 623.
[16] C. Alix-Panabières, K. Pantel, *Lab Chip* **2014**, *14*, 57.
[17] S. Riethdorf, L. O'Flaherty, C. Hille, K. Pantel, *Adv. Drug Delivery Rev.* **2018**, *125*, 102.
[18] C. Alix-Panabières, S. Mader, K. Pantel, *J. Mol. Med.* **2017**, *95*, 133.
[19] C. L. Chaffer, B. P. San Juan, E. Lim, R. A. Weinberg, *Cancer Metastasis Rev.* **2016**, *35*, 645.
[20] F. Brinkmann, M. Hirtz, A. Haller, T. M. Gorges, M. J. Vellekoop, S. Riethdorf, V. Müller, K. Pantel, H. Fuchs, *Sci. Rep.* **2015**, *5*, 15342.
[21] F. Huo, Z. Zheng, G. Zheng, L. R. Giam, H. Zhang, C. A. Mirkin, *Science* **2008**, *321*, 1658.
[22] R. D. Piner, J. Zhu, F. Xu, S. Hong, C. A. Mirkin, *Science* **1999**, *283*, 661.
[23] D. J. Eichelsdoerfer, X. Liao, M. D. Cabezas, W. Morris, B. Radha, K. A. Brown, L. R. Giam, A. B. Braunschweig, C. A. Mirkin, *Nat. Protoc.* **2013**, *8*, 2548.
[24] L. R. Giam, M. D. Massich, L. Hao, L. Shin Wong, C. C. Mader, C. A. Mirkin, *Proc. Natl. Acad. Sci. USA* **2012**, *109*, 4377.
[25] R. Kumar, A. Urtizberea, S. Ghosh, U. Bog, Q. Rainer, S. Lenhert, H. Fuchs, M. Hirtz, *Langmuir* **2017**, *33*, 8739.
[26] Z. Zheng, W. L. Daniel, L. R. Giam, F. Huo, A. J. Senesi, G. Zheng, C. A. Mirkin, *Angew. Chem., Int. Ed.* **2009**, *48*, 7626.
[27] F. Brinkmann, M. Hirtz, A. M. Greiner, M. Weschenfelder, B. Waterkotte, M. Bastmeyer, H. Fuchs, *Small* **2013**, *9*, 3265.
[28] G. Arrabito, H. Schroeder, K. Schröder, C. Filips, U. Marggraf, C. Dopp, M. Venkatachalapathy, L. Dehmelt, P. I. H. Bastiaens, A. Neyer, C. M. Niemeyer, *Small* **2014**, *10*, 2870.
[29] R. Kumar, S. Weigel, R. Meyer, C. M. Niemeyer, H. Fuchs, M. Hirtz, *Chem. Commun.* **2016**, *52*, 12310.
[30] R. Kumar, A. Bonicelli, S. Sekula-Neuner, A. C. B. Cato, M. Hirtz, H. Fuchs, *Small* **2016**, *12*, 5330.
[31] A. D. Stroock, S. K. W. Dertinger, A. Ajdari, I. Mezic, H. A. Stone, G. M. Whitesides, *Science* **2002**, *295*, 647.
[32] S. L. Stott, C. Hsu, D. I. Tsukrov, M. Yu, D. T. Miyamoto, B. A. Waltman, S. M. Rothenberg, A. M. Shah, M. E. Smas, G. K. Korir, F. P. Floyd, A. J. Gilman, J. B. Lord, D. Winokur, S. Springer, D. Irimia, S. Nagrath, L. V. Sequist, R. J. Lee, K. J. Isselbacher, S. Maheswaran, D. A. Haber, M. Toner, *Proc. Natl. Acad. Sci. USA* **2010**, *107*, 18392.
[33] T. P. Forbes, J. G. Kralj, *Lab Chip* **2012**, *12*, 2634.
[34] N. S. Lynn, J. Homola, *Anal. Chem.* **2015**, *87*, 5516.
[35] N. S. Lynn, M. Bocková, P. Adam, J. Homola, *Anal. Chem.* **2015**, *87*, 5524.
[36] A. Grimmer, X. Chen, M. Hamidović, W. Haselmayr, C. L. Ren, R. Wille, *RSC Adv.* **2018**, *8*, 34733.
[37] G. E. E. Hvichia, Z. Parveen, C. Wagner, M. Janning, J. Quidde, A. Stein, V. Müller, S. Loges, R. P. L. Neves, N. H. H. Stoecklein, H. Wikman, S. Riethdorf, K. Pantel, T. M. T. M. Gorges, *Int. J. Cancer* **2016**, *138*, 2894.
[38] M. C. Miller, P. S. Robinson, C. Wagner, D. J. O'Shannessy, *Cytometry, Part A* **2018**, *93*, 1234.
[39] J. Chudziak, D. J. Burt, S. Mohan, D. G. Rothwell, B. Mesquita, J. Antonello, S. Dalby, M. Ayub, L. Priest, L. Carter, M. G. Krebs, F. Blackhall, C. Dive, G. Brady, *Analyst* **2016**, *141*, 669.
[40] Z. Shen, A. Wu, X. Chen, *Chem. Soc. Rev.* **2017**, *46*, 2038.
[41] N. H. Stoecklein, J. C. Fischer, D. Niederacher, L. W. M. M. Terstappen, *Expert Rev. Mol. Diagn.* **2016**, *16*, 147.
[42] L. Cayrefourcq, T. Mazard, S. Joosse, J. Solassol, J. Ramos, E. Assenat, U. Schumacher, V. Costes, T. Maudelonde, K. Pantel, C. Alix-Panabières, *Cancer Res.* **2015**, *75*, 892.
[43] Y. Su, T. J. Pogash, T. D. Nguyen, J. Russo, *Cancer Med.* **2016**, *5*, 558.
[44] M. Yu, A. Bardia, N. Aceto, F. Bersani, M. W. Madden, M. C. Donaldson, R. Desai, H. Zhu, V. Comaills, Z. Zheng, B. S. Wittner, P. Stojanov, E. Brachtel, D. Sgroi, R. Kapur, T. Shioda, D. T. Ting, S. Ramaswamy, G. Getz, A. J. Iafrate, C. Benes, M. Toner, S. Maheswaran, D. A. Haber, *Science* **2014**, *345*, 216.
[45] A. Franken, C. Driemel, B. Behrens, F. Meier-Stiegen, V. Endris, A. Stenzinger, D. Niederacher, J. C. Fischer, N. H. Stoecklein, E. Ruckhaeberle, T. Fehm, H. Neubauer, *Clin. Chem.* **2019**, *65*, 549.
[46] S. Wang, K. Liu, J. Liu, Z. T.-F. Yu, X. Xu, L. Zhao, T. Lee, E. K. Lee, J. Reiss, Y.-K. Lee, L. W. K. Chung, J. Huang, M. Rettig, D. Seligson, K. N. Duraiswamy, C. K.-F. Shen, H.-R. Tseng, *Angew. Chem., Int. Ed.* **2011**, *50*, 3084.
[47] H. J. Yoon, T. H. Kim, Z. Zhang, E. Azizi, T. M. Pham, C. Paoletti, J. Lin, N. Ramnath, M. S. Wicha, D. F. Hayes, D. M. Simeone, S. Nagrath, *Nat. Nanotechnol.* **2013**, *8*, 735.
[48] W. Sheng, O. O. Ogunwobi, T. Chen, J. Zhang, T. J. George, C. Liu, Z. H. Fan, *Lab Chip* **2014**, *14*, 89.
[49] Y. Song, Y. Shi, M. Huang, W. Wang, Y. Wang, J. Cheng, Z. Lei, Z. Zhu, C. Yang, *Angew. Chem., Int. Ed.* **2019**, *58*, 2236.
[50] B. J. Kirby, M. Jodari, M. S. Loftus, G. Gakhar, E. D. Pratt, C. Chanel-Vos, J. P. Gleghorn, S. M. Santana, H. Liu, J. P. Smith, V. N. Navarro, S. T. Tagawa, N. H. Bander, D. M. Nanus, P. Giannakakou, *PLoS One* **2012**, *7*, e35976.
[51] K. Yoneda, T. Kuwata, Y. Chikaishi, M. Mori, M. Kanayama, M. Takenaka, S. Oka, A. Hirai, N. Imanishi, K. Kuroda, Y. Ichiki, T. Ohnaga, F. Tanaka, *Cancer Sci.* **2019**, *110*, 726.
[52] J. Jiang, H. Zhao, W. Shu, J. Tian, Y. Huang, Y. Song, R. Wang, E. Li, D. Slamon, D. Hou, X. Du, L. Zhang, Y. Chen, Q. Wang, *Sci. Rep.* **2017**, *7*, 42612.
[53] C. V. Pecot, F. Z. Bischoff, J. A. Mayer, K. L. Wong, T. Pham, J. Bottsford-Miller, R. L. Stone, Y. G. Lin, P. Jaladurgam, J. W. Roh,

B. W. Goodman, W. M. Merritt, T. J. Pircher, S. D. Mikolajczyk, A. M. Nick, J. Celestino, C. Eng, L. M. Ellis, M. T. Deavers, A. K. Sood, *Cancer Discovery* **2011**, *1*, 580.

[54] D. Issadore, J. Chung, H. Shao, M. Liong, A. A. Ghazani, C. M. Castro, R. Weissleder, H. Lee, *Sci. Transl. Med.* **2012**, *4*, 141ra92.

[55] E. Ozkumur, A. M. Shah, J. C. Ciciliano, B. L. Emmink, D. T. Miyamoto, E. Brachtel, M. Yu, P.-I. Chen, B. Morgan, J. Trautwein, A. Kimura, S. Sengupta, S. L. Stott, N. M. Karabacak, T. A. Barber, J. R. Walsh, K. Smith, P. S. Spuhler, J. P. Sullivan, R. J. Lee, D. T. Ting, X. Luo, A. T. Shaw, A. Bardia, L. V. Sequist, D. N. Louis, S. Maheswaran, R. Kapur, D. A. Haber, M. Toner, *Sci. Transl. Med.* **2013**, *5*, 179ra47.

[56] S. Ribeiro-Samy, M. I. Oliveira, T. Pereira-Veiga, L. Muinelo-Romay, S. Carvalho, J. Gaspar, P. P. Freitas, R. López-López, C. Costa, L. Diéguez, *Sci. Rep.* **2019**, *9*, 8032.

[57] R. C. Team, R: A language and environment for statistical computing,https://www.r-project.org (accessed: November 2019).

[58] D. J. Benjamin, J. O. Berger, M. Johannesson, B. A. Nosek, E.-J. Wagenmakers, R. Berk, K. A. Bollen, B. Brembs, L. Brown, C. Camerer, D. Cesarini, C. D. Chambers, M. Clyde, T. D. Cook, P. De Boeck, Z. Dienes, A. Dreber, K. Easwaran, C. Efferson, E. Fehr, F. Fidler, A. P. Field, M. Forster, E. I. George, R. Gonzalez, S. Goodman, E. Green, D. P. Green, A. G. Greenwald, J. D. Hadfield, et al., *Nat. Hum. Behav.* **2018**, *2*, 6.